Researchers Journal of Science and Technology (REJOST)

Estimation of aquifer geohydrodynamic properties using the Inverse Slope method

Aniekan M. Ekanem

Received: 15 October 2021 / Accepted: 30 November 2021

Abstract

This study is aimed at estimating aquifer geohydrodynamic properties of the hinterland aquifers of Obot Akara Local Government area for groundwater development in the area. A total of 12 Vertical Electrical Soundings (VES) was conducted in the area with the use of the Schlumberger electrode configuration with maximum current electrode separation of 600 m. The acquired data were interpreted using the modified Inverse Slope Method (ISM) to obtain the primary geoelectric parameters of the various lithological and hydrogeological units penetrated by the current in the area. The area is shown to comprise 3 to 4 geoelectric layers, with the third layer constituting the economical exploitable aquifer. The thickness of this layer varies from 54.4 to 129.5 m with an average value of 86.7 m while its bulk resistivity varies from 396.0 to 3333.3 Ωm with an average value of 1425.5 Ωm. These two primary aquifer parameters were used in conjunction with empirical relations in literature to estimate the geohydrodynamic properties of the hinterland aquifers in the area. The estimated properties are pointers to the fact that aquifers in the area are very productive.

Keywords Aquifer; Geohydrodynamic Properties; Inverse Slope; Groundwater; Resistivity

✉ Aniekan M. Ekanem
anny4mart@yahoo.com;
aniekanekanem@aksu.edu.ng

Department of Physics, Geophysics Research Group (GRG), Akwa Ibom State University, Ikot Akpaden, Mkpat Enin, Nigeria

1.0 Introduction

Aquifer geohydrodynamic properties are very essential parameters in groundwater resources development and management (Soupios *et al.*, 2005; George *et al.*, 2017). These properties include porosity, formation factor, hydraulic conductivity or coefficient of permeability, transmissivity, permeability and tortuosity. The subsurface of the earth comprises rock types with characteristic porosity and permeability. To act as a good aquifer, the rock in the aquifer

must have good porosity in terms of connectivity of the available pore spaces and permeability. Porosity is a measure of the void spaces in a rock. Groundwater exists in the pore spaces between grains of soil and rocks. The geometry and connectivity of the pore spaces affect the rock permeability and hence groundwater flow (Freeze and Cherry, 2002). Groundwater flow in soils and rocks is controlled by the hydraulic characteristics of the shape and size of pore spaces (Uwa *et al*., 2018; Ibuot and Obiora, 2020). In a given rock unit, the effective porosity and permeability constitute the controlling factors in groundwater manage-ment (Abed 2014; George *et al*., 2017). Among the factors affecting rock per-meability are pore geometry or configuration, grain shape and size, cementation factor, rock type, degree of saturation, diagenetic process and of course the depositional environment (Abuseda *et al*., 2015). Tortuosity depends on permeability and hydraulic conductivity or coefficient of permeability. High tortuosity leads to low effective porosity and hence low permeability (George et al. 2011). Transmissivity and hydraulic conductivity are closely related and both govern the flow of groundwater through the aquifer (Freeze and Cherry, 2002). They both describe the general capability of an aquifer to transmit water over the whole saturated thickness and unit thickness respectively.

Permeability information is often accessible from laboratory measurement in core plugs (George *et al*., 2017). Aquifer hydraulic conductivity and transmissivity could be estimated from pumping test results, grain size analysis and permeability measurements (Sattar *et al*., 2016; Ekanem et al 2020). However, estimating these parameters from pumping tests and downhole well data could be too expensive, labour intensive and time consuming and in most cases, it is difficult to obtain realistic core materials by drilling (George et al., 2017; Ekanem et al 2020). As a result of geologic heterogeneity, aquifer hydrodynamic properties interpolated between few boreholes that may be available in an area could be erroneous particularly those that are far away from the borehole site *(*Niwas *et al.*, 2011*;* Ekanem *et. al.*, 2020*).* To overcome these challenges, the surface resistivity method has proven to be very useful (Niwas *et al.*, 2011*;* Uwa *et al*., 2018; George *et al*., 2017; Ekanem *et. al.*, 2020*;* Ibuot and Obiora, 2020). The method allows the estimation of the aquifer primary geoelectric parameters (thickness, bulk resistivity), which could be used in conjunction with established relationships in literature to estimate these important hydrodynamic properties. Aside saving cost and time, the surface resistivity method is non-invasive and very friendly with the environment.

This study involves the use of the surface resistivity method to estimate the important aquifer geohydrodynamic properties in Obot Akara Local Government area. Prior to the creation of the local government area in 1996, the inhabitants of the area were wholly dependent on surface water sources (streams) for their domestic and agricultural needs. The attendant effect of the creation of the local government is a geometric growth of popu-lation and micro-industrial activities in the area and eventually an increase in the water needs of the people. Over the years, the area has experienced a decline in surface water quality and increasing demand for groundwater due to population growth among other factors. The major aim of this study therefore is to determine the aquifer geohydrodynamic properties, which will facilitate the development of an effective and sustainable groundwater management scheme in the area.

2.0 Location and geology of the study area

This study was undertaken in Obot Akara Local Government area, which lies between latitudes 4°55′ N and 5°00′ N and longitudes 7°30′ E and 7°40′ E in the eastern part of the Niger Delta, southern Nigeria (Fig. 1). Obot Akara Local Government area in Akwa Ibom State, covers an area of about 237 km^2 and is accessible through a network of roads and is bordered by Ini Local Government area and parts of Abia State on the northern side; Ikot Ekpene and Ikono local government area on the eastern side; Essien Udim local government area on the southern side and also part of Abia state on the western side.

The area generally has a land surface of very little or no significant relief over several kilometres.

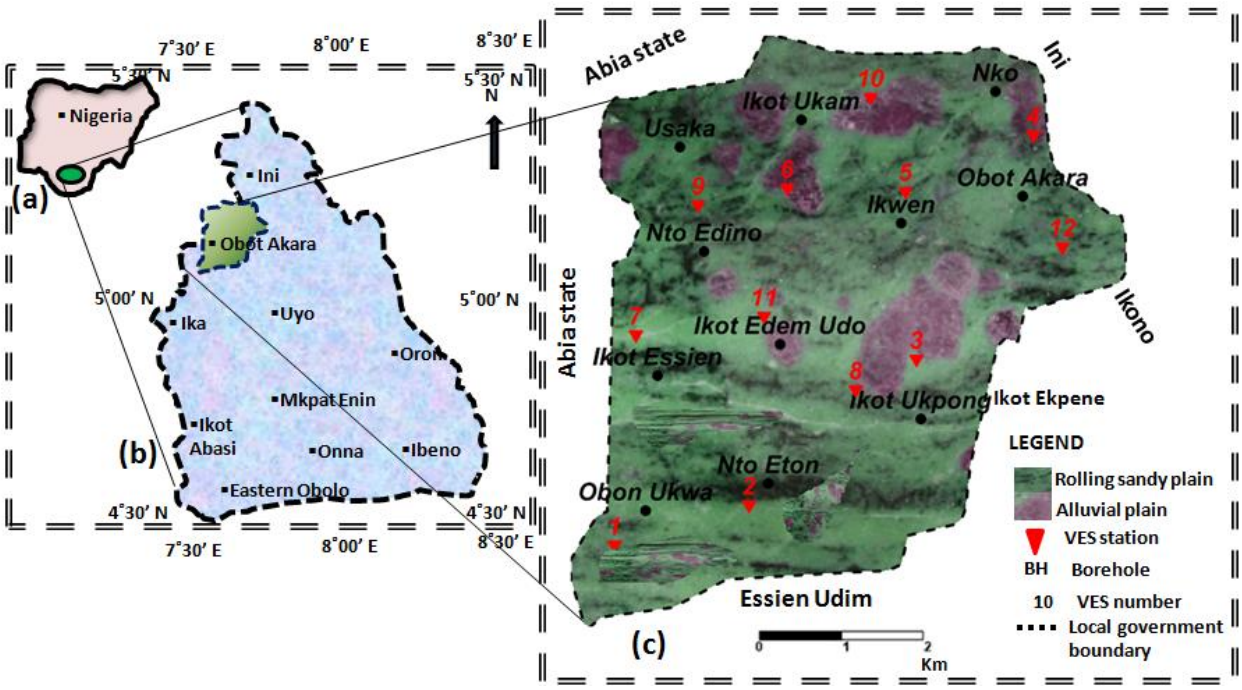

Fig. 1: Schematic map showing location of study area and sounding stations (a) Nigeria showing Akwa Ibom State (b) Akwa Ibom State showing the study area (c) Study area and its geology

In terms of climate, Obot Akara is characterized by two distinctive seasons, which are the rainy and dry seasons with an annual rainfall of about 2289 mm and average annual temperature of 26.2°C respectively and is drained by the Kwa Ibo River and its tributaries (Ekanem *et al*., 2021).

Geologically, the major sediments covering Obot Akara County are recent - to - Tertiary sands, which belong to the Benin Formation (otherwise referred to as Coastal Plain sands - CPS). The Benin formation is the uppermost part of the Niger Delta, comprising mainly sands and gravels and constitutes the major hydrogeological units in the area. The sands are poorly sorted with grain sizes ranging from fine to coarse (Short and Stauble 1967, Mbipom et al. 1996). In addition, slight intercalations of lignite, clays, sandstone and silts occur at several places in the area (Reijers *et al*., 1987). A multi-aquifer system is built up at a number of places as a result of alternations of sand and clay at those places (Okereke *et al*., 1998; Esu *et al*., 1999; Edet and Okereke 2002). The CPS is underlain by the Agbada Formation, which is the major hydrocarbon bearing unit in the Niger Delta region (Short and Stauble, 1967; Avbovbo, 1978; Stacher, 1995).

3.0 Theoretical foundations

3.1 Aquifer hydrodynamic properties

Aquifer hydrodynamic properties provide indispensable information about the behaviour of the aquifer and also help in the development of qualitative demarcations and analytical models, which are very vital in groundwater management and exploitation. These properties include porosity, formation factor, hydraulic conductivity or coefficient of permeability, transmissivity, permeability and tortuosity.

Porosity and Formation factor

Porosity (symbol φ), which is usually expressed as a percentage is the ratio of the volume of pores to the volume of bulk rock. The aquifer storage capacity is determined by porosity. Porosity of sedimentary rocks is dependent on the grain size, shapes of the grains, degree of sorting and cementation. Porosity can be estimated from the formation factor F by the use of Archie's equation (Archie 1942) given in Eq. 1.

$$F = \frac{\rho_b}{\rho_w} = a\phi^{-m} \qquad (1)$$

where ρ_b is the aquifer bulk resistivity, ρ_w is the resistivity of water, m represents the cementation exponent, a the pore geometrical factor and F is the formation factor of clay-free, clean, consolidated sediments.

Hydraulic conductivity or coefficient of permeability

Hydraulic conductivity K is a fundamental factor which affects the flow of groundwater through a given aquifer. It could be defined as the ability of the aquifer to transmit water under the effect of hydraulic gradient (Lobo Ferreira *et al.*, 2005). Aquifer hydraulic conductivity in general is determined by the use of the Kozeny-Carmen-Bear's model equation given in Eq. 2 (Domenico, and Schwartz, 1990).

$$K \approx \left(\frac{\delta_w g}{\mu_d}\right).\left(\frac{d_m{}^2}{180}\right).\left(\frac{\phi^3}{(1-\phi)^2}\right) \qquad (2)$$

where δ_w is the density of water, d_m is the mean grain size of sediments and μ_d is the dynamic viscosity of water. The rate of groundwater flow depends on the hydraulic conductivity and hydraulic gradient. The greater the hydraulic conductivity or a porous medium, the more rapid groundwater flows through it.

Permeability

Permeability is the property a rock has to transmit fluids. It is related to porosity but is not always dependent upon it. Permeability is controlled by the size of the connecting passages (pore throats or capillaries) between pores. The permeability of an aquifer is related to its hydraulic conductivity and water dynamic viscosity according to Eq. 3:

$$K_p = \frac{K\mu_d}{\delta_w g} \qquad (3)$$

The Concept of permeability is important in groundwater studies because it determines the flow characteristics of groundwater in the aquifers. High permeability implies that groundwater can move swiftly through the aquifer. Effective porosity and permeability are the major factors controlling groundwater abstraction in stratigraphically neighbouring hydrogeological units (George et al., 2017).

Transmissivity

Transmissivity (T) is a crucial transmission property, which expresses the ability of the aquifer to transmit water throughout its entire system (Freeze and Cherry 1979). It could be defined as the rate of groundwater flow under unit hydraulic gradient through a cross-section of unit width over the total saturated thickness of the aquifer (Bear, 1979; Kruseman and de Ridder, 1990). Transmissivity depends on the shape, amount, and interconnectivity of void

spaces, or permeability structure. Transmissivity T is related with hydraulic conductivity through Eq. 4 (Niwas and Singhal, 1981):

$$T = Kh \quad (4)$$

where h is the thickness of the layer. Transmissivity compared with hydraulic conductivity includes the entire saturation thickness of the aquifer while hydraulic conductivity is defined only for a unit saturation thickness. High aquifer transmissivity corresponds to high groundwater potential and vice versa.

Tortuosity

Tortuosity is an inherent property of a porous material and is defined as the ratio of the length of the flow path to the straight-line distance between the ends of the flow path (Bear, 1979). Tortuosity is related with fractional porosity and formation factor through Eq. 5.

$$\tau = \sqrt{F\phi} \quad (5)$$

3.2 The Inverse Slope Method (ISM)

The inverse slope method was introduced by Sankarnaryan and Ramanujachary (1967) for the interpretation of sounding data using the Wenner array. In this method, the the inverse of the resistance is plotted as abscissa against the constant electrode spacing 'a'. The number of the linear segments identified on the graph corresponds to the number of layers penetrated by current. The slope of each segments of the graph gives the true resistivity of the layer while the intersections of the segments give the depth of the layer respectively.

ISM can be modified for use in the interpretation of sounding data obtained using the Schlumberger array (Kouassi *et al.,* 2017*;* Bouadou *et al.*, 2019). From the acquired data, the values of $\frac{AB}{2}\Big/\rho_a$ are plotted against AB/2 for each sounding station to generate a graph with linear segments corresponding to the number of layers (Fig. 2.0). The magnitude of the inverse of the slopes of the various segments gives the true resistivity of the respective layers while the thicknesses can be obtained from the intersections of the segments. The true resistivity of the first layer, for instance is given by Eq. 6:

$$\rho_1 = \frac{1}{|a_1|} \quad (6)$$

where a_1 the slope of the first linear segment. The depth to the various interfaces is given in general by Eq. 7:

$$x_n = \frac{(b_{n+1} - b_n)}{(a_n - a_{n+1})} \times \frac{2}{3} \quad (7)$$

where *a* and *b* are the respective slopes and intercepts of the linear segments while n is the number of segments, which corresponds to the number of layers. The thickness of each layer (H) is the difference between the depths of two successive layers. The inverse slope method is easy to use for interpretation of surface resistivity data as the standard curves are not required and it usually gives reasonably good results (Bouadou *et al.*, 2019.

4.0 Materials and method

In this study, vertical electrical sounding (VES) was carried out in twelve communities in the study area as indicated in Fig. 1 using the Schlumberger array. The major field equipment was the ABEM terrameter (SAS 1000 model), which injects a well-defined current into the ground through two electrodes planted on the earth surface (current electrodes A and B) and detects the generated potential difference by means of two other surface electrodes (potential electrodes M and N). Maximum current electrode separation (AB) was 600 m. The terrameter gives the apparent resistance of the earth layers penetrated by the current as the

output. Two of the soundings were made in the neighbourhood of two existing boreholes in the area where the available borehole data were used as controls especially in the delineation of the various litho units during the data interpretation.

First, the raw apparent resistance (R_a) measured in the field was first converted into apparent resistivity ρ_a by using Eq. (8):

$$\rho_a = G_f * R_a \quad (8)$$

where G_f is referred to as the geometric factor, which for the Schlumberger array depends on the distance between the current electrodes (AB) and potential electrodes (MN) respectively according to Eq. (9):

$$G_f = \pi * \left\{ \frac{\left(\frac{AB}{2}\right)^2 - \left(\frac{MN}{2}\right)^2}{MN} \right\} \quad (9)$$

Next, the modified ISM proposed by Sankarnaryan and Ramanujachary (1967) was used to interpret the data to obtain the primary geoelectric layer parameters of the various lithological and hydrogeological units in the area. For each sounding station, the values of $\frac{AB}{2}\Big/\rho_a$ were computed and plotted against AB/2. The slopes of the respective segments correspond to the inverse of the true layer resistivity while the number of segments corresponds to the number of layers. The depths of each of the layers were computed by using Eq. (7), from where the thicknesses were computed. The linear equations of the various segments had a coefficient of determination (R^2) of between 0.85 and 0.99 for all the soundings stations. Sample plots of these graphs are shown in Fig. 3.0. The layer thicknesses and resistivities obtained were taken to represent the true subsurface models of the study area.

4.1 Results, Analysis and Discussion

The result of VES data interpretations shows that the study area is made up of 3 to 4 geoelectric layers within the permissible limit of the utilized maximum current electrode spacing as summarized in Table 1.0. The first layer, which cuts across the whole study area, has resistivity range from 64.6 to 1883.2 Ωm with an average value of 760.2 Ωm. This layer was interpreted as the motley topsoil and has a thickness varying from 1.9 m to 19.7 m with an average value of 7.2 m. The resistivity variations observed in this motley topsoil may be due to the artificial nature of the layer coupled with the ongoing bioturbating activities in the layer (George et al. 2017; Ekanem, 2020). The second layer has resistivity values ranging from 123.5 to 2762.4 Ωm and thickness varying from 5.6 to 84.8 m. The mean values of resistivity and thickness of this layer are 1069.2 Ωm and 39.5 m respectively. The observed variations in resistivity values of this layer, interpreted to be fine or medium grained sands at some communities and sandy clay or gravelly sands at other communities (as summarized in Table 1.0) may be attributed to the varying grain sizes of the geomaterials of this layer (Ekanem *et al.*, 2020). The second layer has resistivity values ranging from 123.5 to 2762.4 Ωm and thickness varying from 5.6 to 84.8 m. The mean values of resistivity and thickness of this layer are 1069.2 Ωm and 39.5 m respectively. The observed variations in resistivity values of this layer, interpreted to be fine or medium grained sands at some communities and sandy clay or gravelly sands at other communities (as summarized in Table 1.0) may be attributed to the varying grain sizes of the geomaterials of this layer (Ekanem *et al.*, 2020). The third geoelectric layer has resistivity values ranging from 396.0 to 3333.3 Ωm with an average value of 1425.5 Ωm while its thickness ranges from 54.4 to 129.5 m with an average value of 86.7 m.

Again, this layer was interpreted to be gravelly sands at some locations or coarse sands at other locations as summarized in Table 1.0. This geoelectric layer forms the major exploitable aquifer in the area. The fourth and of course the last identifiable geoelectric layer in some communities (Ubon Ukwa, Nto Eton, Mbat Esifon, Ikwen, Abiakpo Ikot Ukam and Ikot Essien) has resistivity values ranging from 666.7 to 1666.7 Ωm with an average value of 1101.9 Ωm. The depth or thickness of this layer could not be ascertained as the current could not get to the bottom of the layer with the maximum current electrodes used. The delineation of the various litho units in the area from the results of the VES inter-pretation was constrained by the available information from two boreholes in the area. The distribution of the aquifer bulk resistivity ρ_b is shown in the image map of Fig. 4.0. Relatively, low resistivity values of 396.0 to 1000.0 Ωm are noticed in some communities in the western and northeastern parts of the study area as shown in Fig. 4.0 (a). This may indicate poor groundwater quality in these communities.

Determination of aquifer hydrodynamic properties

To estimate the aquifer hydrodynamic properties, first the water resistivity needs to be known. In this study, the water resistivity was estimated using the empirical relation derived by Ibanga and George (2016) for aquifers of similar geomaterials (Eq. 10).

$$\rho_w = 0.05777\rho_b + 13.643 \qquad (10)$$

The distribution of the water resistivity is shown in Fig. 4. 0(b). A comparison of Figs. 4 .0 (a) and (b) shows that areas of low aquifer bulk resistivity also correspond to areas with low water resistivity as a consequence of Eq. 10. In all, six aquifer hydrodynamic properties were estimated from the interpreted VES results using the relevant equations given in section 3.1.

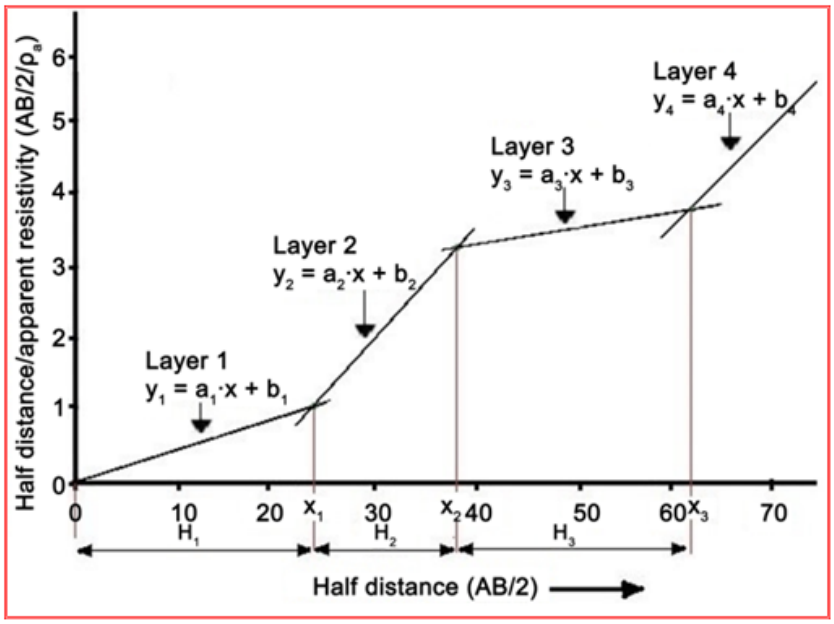

Fig. 2.0: Graph of modified Inverse Slope method for Schlumberger array (adapted from Bouadou et al., 2019)

These properties are the porosity, formation factor, hydraulic conductivity, transmissivity, permeability and tortuosity. The average values of the pore geometry factor *a* = *0.5245*, cementation exponent m = 1.5431 and mean grain size d_m of 0.000348m (George et al., 2011) and George et al., 2015) were used to determine the aquifer porosity and the hydraulic conductivity. The dynamic viscosity of water was taken as 0.0014 kg/ms (Fetters, 1994) while 1000 kg/m^3 was used for the density of water.

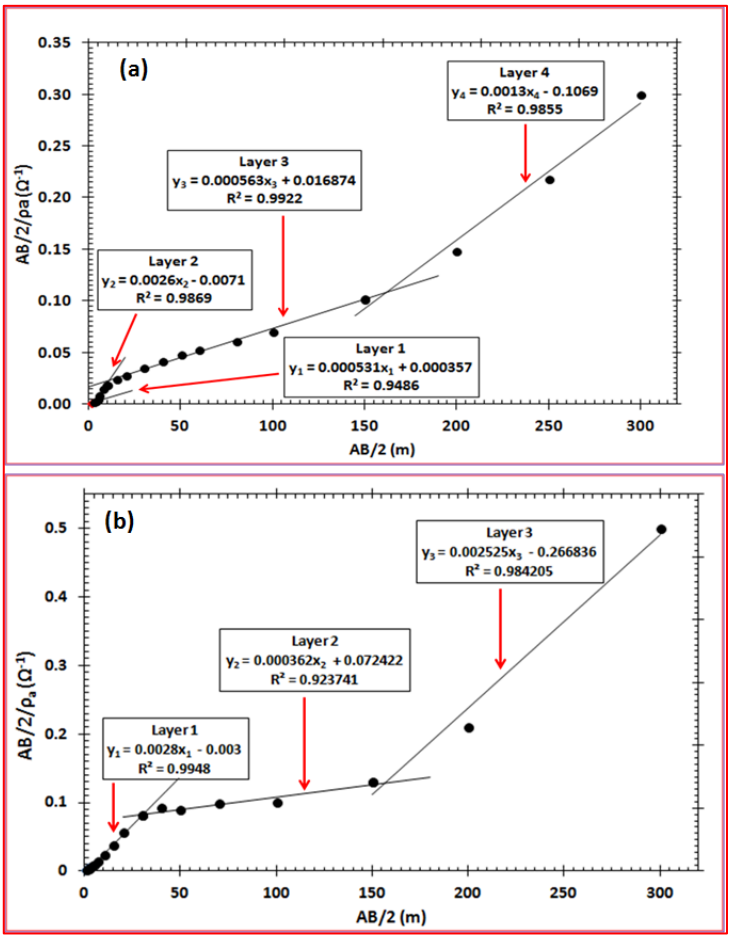

Fig. 3.0: Sample graphs for the analysis of Inverse Slope method (a) VES 2 at Nto Eton (b) VES 10 at Utu Ikot Inyang

Details of the computed aquifer properties are shown in Table 2.0. The formation factor varies from 14.2 to 27 while the porosity values vary from 7.8 to 11.8%. Fig. 5.0 shows the distribution of the porosity and formation factor in the study area. The distributions of both parameters are similar as is expected from Eq. 5 and both depend on lithology. Low porosity values of nearly 8% observed in Ikot Essien and Ikot Ukpong communities indicate that the aquifers in these communities composed of fine sands while the very nearly constant value of 11 % observed in the other communities indicates aquifer comprising gravelly sands. The hydraulic conductivity k varies from 0.19 to 0.67 m/day with an average value of 0.54 m/day while the transmissivity has a range of 10.5 to 67.8 m^2 /day with an average value of 42.1 m^2/day. The image maps of Fig. 6.0 show the distribution of the hydraulic conductivity and transmissivity. Again, low values of these two parameters are observed respectively in Ikot Essien and Ikot Ukpong communities. The aquifer permeability varies between 321.9 and 1130.2 mD with an average value of 898.8 mD while tortuosity varies from 1.29 to 1.45 with an average value of 1.33. The image maps of Fig. 7.0 shows the distribution of permeability and tortuosity in the study area. The distribution map of permeability (Fig. 7.0 (a) is the inversion of that of tortuosity (Fig. 7.0 (b).

Table 1.0: Summary of VES interpretation

VES No.	Location Name	Longitude (Degrees)	Latitude (Degrees)	No. of Layers	Resistivity (Ωm)	Thickness (m)	Depth (m)	Lithology
1	Ubon Ukwa	7.5588	5.1918	4	1428.6	1.9	1.9	Motley topsoil
					833.3	7.9	9.8	Fine sand
					1250.0	60.4	70.2	Coarse sand
					666.7			Fine sand
2	Nto Eton	7.5949	5.2026	4	1883.2	2.4	2.4	Motley topsoil
					384.6	5.6	8.0	Fine sand
					1769.9	104.3	112.3	Gravelly sand
					769.2			Coarse sand
3	Mbat Esifon	7.6398	5.2417	4	625.0	10.6	10.6	Motley topsoil
					1428.6	20.7	31.3	Coarse sand
					3333.3	129.5	160.8	Gravelly sand
					1428.6			Coarse sand
4	Abiakpo Ibo	7.6712	5.3019	3	1883.2	9.8	9.8	Motley topsoil
					1111.1	77.0	86.7	Coarse sand
					1872.7			Gravelly sand
5	Ikwen	7.6369	5.2867	4	131.6	2.1	2.1	Motley topsoil
					1112.3	10.8	12.9	Coarse sand
					1487.7	108.1	121.0	Gravelly sand
					1171.0			Coarse sand
6	Abiakpo Ikot Ukam	7.6052	5.2876	4	510.2	2.5	2.5	Motley topsoil
					163.9	7.4	9.9	Sandy clay
					2232.1	63.3	73.2	Gravelly sand
					1666.7			Coarse sand
7	Ikot Essien	7.5645	5.2482	4	714.3	3.2	3.2	Motley topsoil
					123.5	10.1	13.2	Sandy clay
					500.0	54.4	67.6	Fine sand
					909.1			Coarse sand
8	Ikot Ukpong	7.6235	5.2335	3	256.4	9.0	9.0	Motley topsoil
					526.3	65.2	74.1	Fine sand
					1250.0			Coarse sand
9	Nto Edino	7.5812	5.2831	3	833.3	12.9	12.9	Motley topsoil
					2057.6	77.7	90.5	Gravelly sand
					625.0			Fine sand
10	Utu Ikot Inyang	7.6275	5.3119	3	357.1	19.7	19.7	Motley topsoil
					2762.4	84.8	104.6	Gravelly sand
					396.0			Fine sand
11	Ikot Idem Udo	7.5989	5.2532	3	434.2	7.9	7.9	Motley topsoil
					1244.2	67.8	75.7	Coarse sand
					671.9			Fine sand
12	Nto Ekpu Nyanyaha	7.679	5.2718	3	64.6	4.5	4.5	Motley topsoil
					1082.7	38.5	43.0	Coarse sand
					1716.9			Gravelly sand

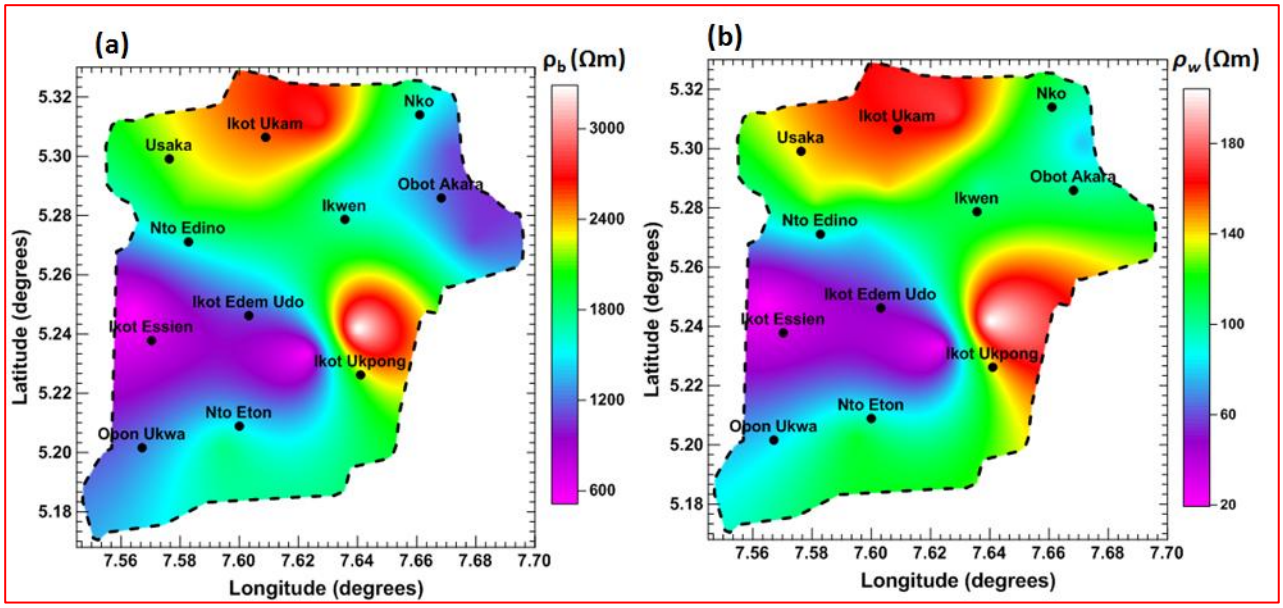

Fig. 4.0: Image map showing (a) distribution of aquifer bulk resistivity (ρ_b) (b) distribution of water resistivity (ρ_w) in the study area

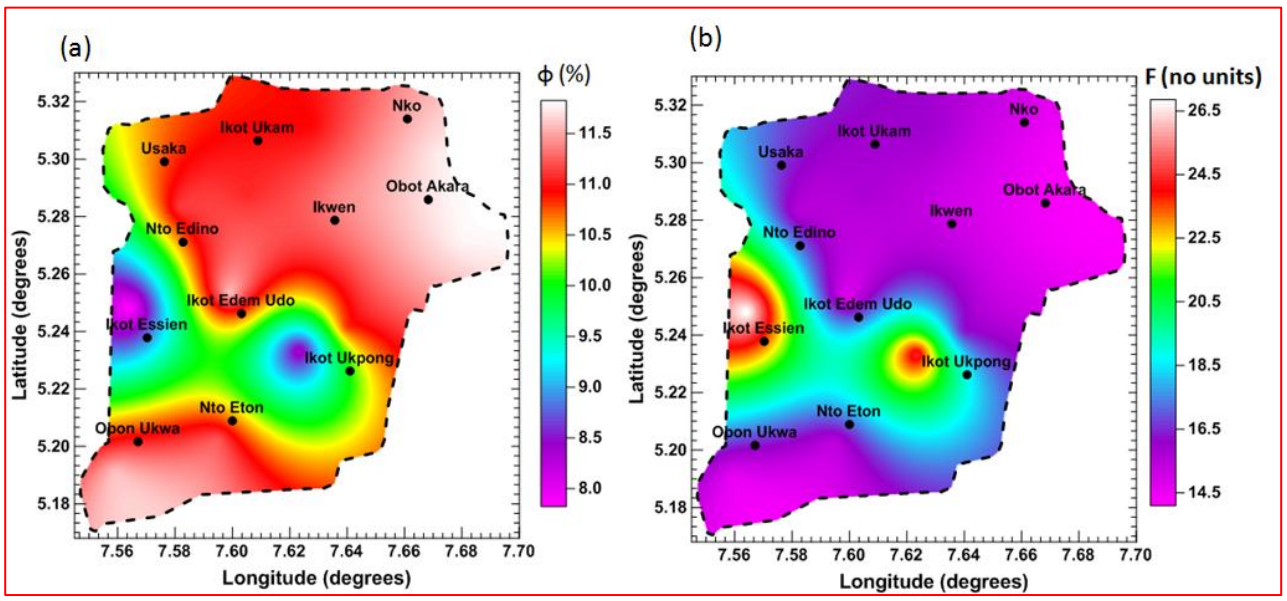

Fig. 5.0: Image map showing (a) distribution of porosity (b) distribution of formation factor in the study area

Table 2.0: Summary of aquifer geohydrodynamic properties

VES No.	Location Name	Bulk resistivity ρ_b (Ωm)	Water resistivity ρ_w (Ωm)	Thickness h (m)	Formation factor F	Porosity ϕ (%)	Hydraulic conductivity K (m/day)	Transmissivity T (m^2/day)	Permeability K_P (mD)	Tortuosity τ
1	Ubon Ukwa	1250.00	85.77	60.40	14.57	11.60	0.64	38.85	1077.63	1.30
2	Nto Eton	1769.91	115.77	104.30	15.29	11.24	0.59	61.07	981.09	1.31
3	Mbat Esifon	3333.33	205.98	129.51	16.18	10.84	0.52	67.84	877.62	1.32
4	Abiakpo Ibo	1111.11	77.75	76.95	14.29	11.75	0.67	51.45	1120.07	1.30
5	Ikwen	1487.65	99.48	108.08	14.95	11.40	0.61	66.10	1024.57	1.31
6	Abiakpo Ikot Ukam	2232.14	142.44	63.31	15.67	11.06	0.56	35.32	934.70	1.32
7	Ikot Essien	500.00	18.50	54.40	27.03	7.77	0.19	10.45	321.94	1.45
8	Ikot Ukpong	526.32	21.40	65.16	24.59	8.26	0.23	15.05	387.05	1.43
9	Nto Edino	2057.61	132.37	77.66	15.54	11.12	0.57	44.02	949.65	1.31
10	Utu Ikot Inyang	2762.43	173.04	84.83	15.96	10.93	0.54	45.64	901.32	1.32
11	Ikot Idem Udo	1244.20	85.43	67.80	14.56	11.60	0.64	43.67	1079.20	1.30
12	Nto Ekpu Nyanyaha	1082.70	76.11	38.50	14.22	11.78	0.67	25.97	1130.21	1.29
	Minimun value	500.00	18.50	38.50	14.22	7.77	0.19	10.45	321.94	1.29
	Maximum value	3333.33	205.98	129.51	27.03	11.78	0.67	67.84	1130.21	1.45
	Average value	1613.12	102.84	77.57	16.91	10.78	0.54	42.12	898.75	1.33

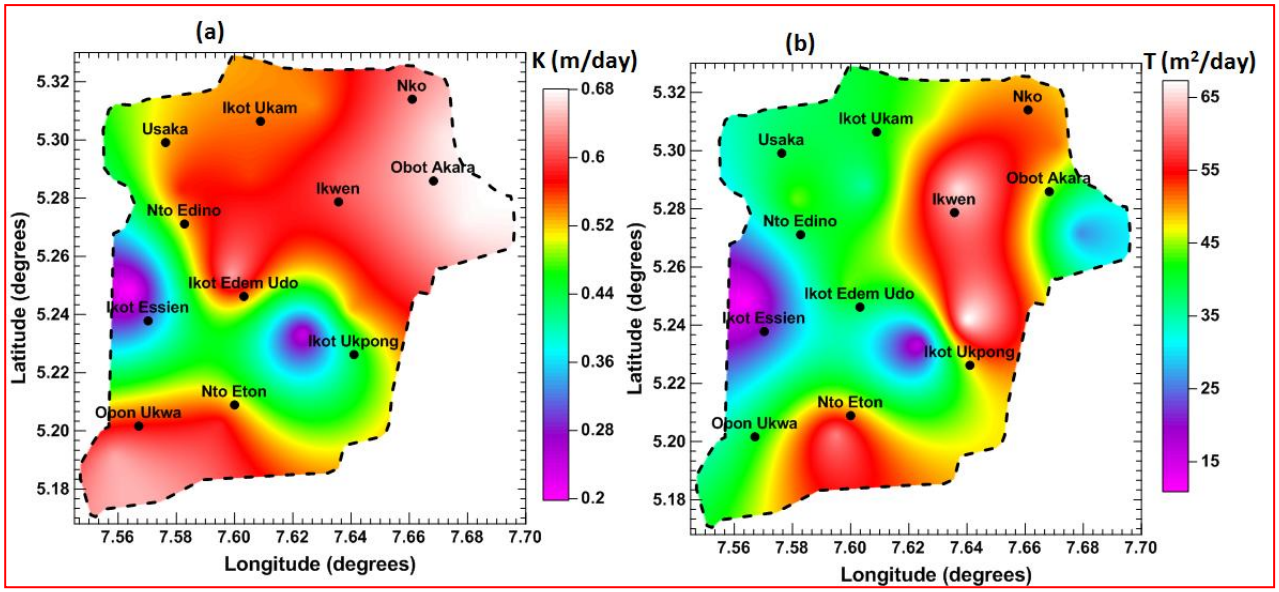

Fig. 6.0: Image map showing (a) distribution of aquifer hydraulic conductivity K (b) distribution of aquifer transmissivity T in the study area

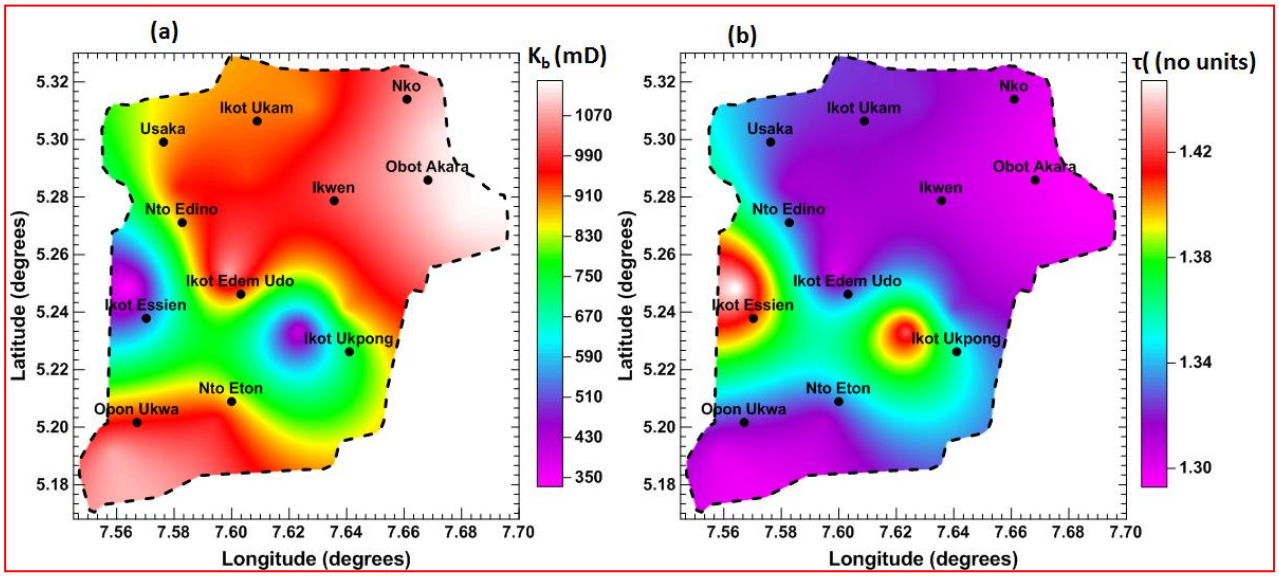

Fig. 7.0: Image map showing (a) distribution of aquifer permeability K_b (b) distribution of aquifer tortuosity (τ) in the study area

Figure 8.0 shows the regression plot of permeability and porosity. The plot reveals a direct relationship between permeability and porosity of the form given in Eq. 11.

$$K_p = 0.6596\phi^{3.019} \qquad (11)$$

Eq. 11 shows that the permeability increases with increasing porosity. Areas of high permeability imply that groundwater can flow more easily through the aquifer. The regression plot of permeability against tortuosity is shown in Fig. 9.0. The plot reveals an inverse relationship between permeability and tortuosity of the form given in Eq. 12.

$$K_p = 19921\tau^{11.12} \qquad (12)$$

The plot of hydraulic conductivity against formation factor shown in Fig. 10.0 shows an

inverse power relationship between the two parameters.

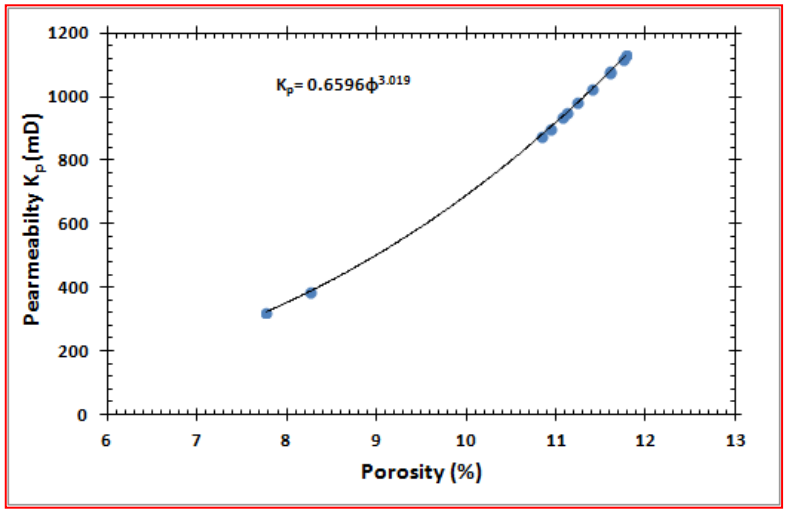

Fig. 8.0: Regression plot of permeability against porosity

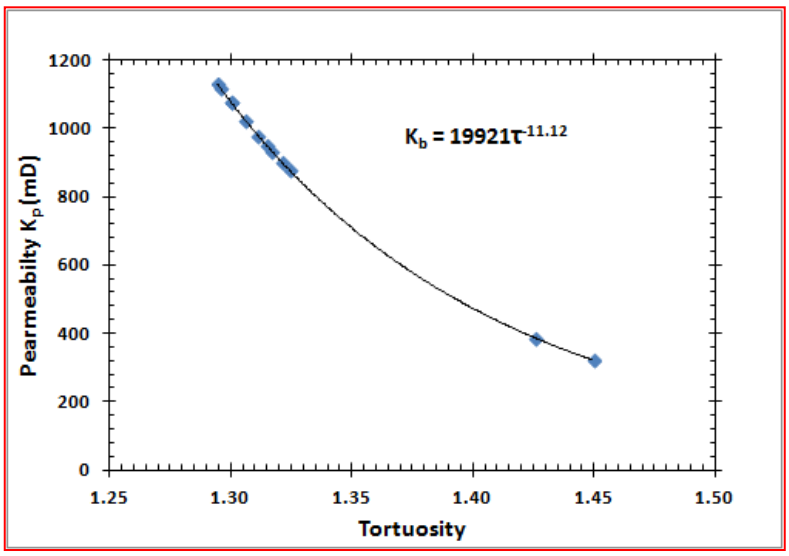

Fig. 9.0: Regression plot of permeability against tortuosity

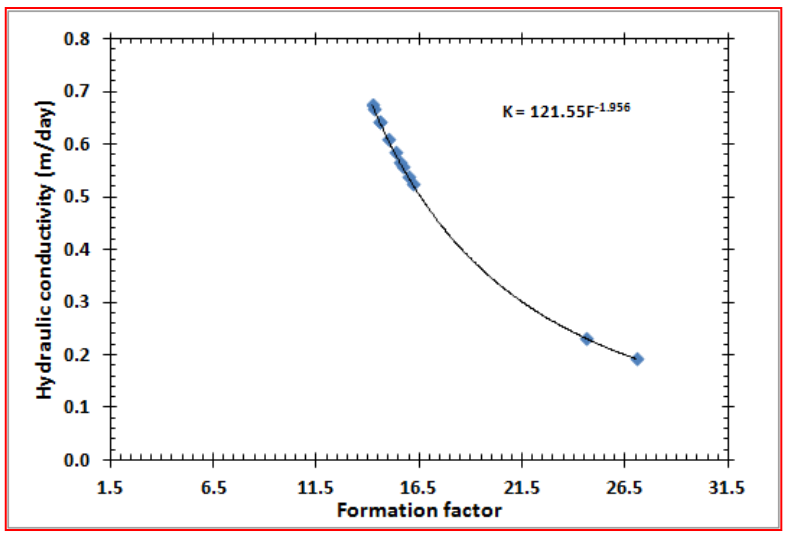

Fig. 10.0: Regression plot of hydraulic conductivity against formation factor

5.0 Summary and concluding remarks

Aquifer geohydrodynamic properties are very vital in groundwater management, development and exploitation. This study demonstrates the applicability of the inexpensive and non-invasive surface resistivity method in determining aquifer geohydrodynamic properties at locations where borehole information is either scare or not available at all. A total of 12 VES was carried out in the area using the Schlumberger electrode configuration with maximum electrode spacing of 600 m. The data obtained were interpreted using the modified ISM proposed by Sankarnaryan and Ramanujachary (1967) to obtain the primary geoelectric layer parameters of the various lithological and hydrogeological units in the area.

These primary parameters were subsequently used in conjunction with empirical relations in literature to estimate the geohydrodynamic properties of the hinterland aquifers of the study area. The general lithology is mainly sands of various sizes ranging from fine-coarse to gravelly sands with few cases of thin clay intercalations at some locations. An inverse relationship exists between porosity and Hydraulic conductivity with formation factor. Areas of low porosity and Hydraulic conductivity correspond to high formation factor. Aquifer permeability increases with porosity but decreases with tortuosity. A linear relationship also exists between hydraulic conductivity and transmissivity. The established empirical relations between hydraulic conductivity and formation factor, permeability and tortuosity and permeability and porosity could be useful in modelling the hydrogeological units for efficient monitoring and managements of groundwater in the area.

Acknowledgements

The author appreciates all the assistance and supports from members of the Geophysics Research Group (GRG), Akwa Ibom State University and Prof A. E. Akpan of the Department of Physics (Applied Geophysics Programme), University of Calabar particularly during the field data acquisition and correction of the original manuscript.

References

Abed, A. A., 2014. Hydraulic flow units and permeability prediction in a carbonate reservoir, Southern Iraq from well log data using non- parametric correlation. *International Journal of Enhanced Research in Science Technology & Engineering* 3(1), 480–486.

Abuseda, H., Kassab, M. A., Lala, A. M. & El Sayed, N. A., 2015. Integrated petrographical and petrophysical studies of some Eocene carbonate rocks, Southwest Sinai, Egypt. *Egyptian Journal of Petroleum*, 24, 213–230

Archie, G. E., 1942. The electrical resistivity log as an aid in determining some reservoir characteristics. *Transactions of the American Institute of Mining, Metallurgical, and Petroleum Engineers*, 146, 54–62.

Avbovbo, A. A., 1978. Tertiary lithostratigraphy of Niger Delta. *Bulletin of American Association of Petroleum Geology*, 62, 297– 306.

Bear, J., 1979. Hydraulics of Groundwater. McGraw-Hill Book Co., New York, 567 pp.

Domenico, P. A., & Schwartz, F. W. 1990. Physical and chemical hydrogeology (p. 324). Hoboken: Wiley Press.

Edet, A. E. & Okereke, C. S. 2002. Delineation of shallow groundwater aquifers in the coastal plain sands of Calabar area

(southern Nigeria) using surface resistivity and hydrogeological data. *Journal of African Earth Sciences*, 35, 433 - 443.

Ekanem, A. M., 2020. Georesistivity modelling and appraisal of soil water retention capacity in Akwa Ibom State University main campus and its environs, Southern Nigeria. *Modelling Earth Systems and Environment*. https://doi.org/10.1007/s40-808-020-00850-6

Ekanem, A. M**.,** George, N. J., Thomas, J. E. and Nathaniel, E. U. 2020. Empirical Relations Between Aquifer Geohydraulic–Geoelectric Properties Derived from Surficial Resistivity Measurements in Parts of Akwa Ibom State, Southern Nigeria. *Natural Resources Research* 29(4), 2635-2646. https://doi.org/10.1007-/s11053-019-09606-1

Ekanem, A. M., Akpan, A. E., George, N. J. and Thomas, J. E., 2021. Appraisal of protectivity and corrosivity of surficial hydrogeological units via geo-sounding measurements. Environ Monit Assess, 193:718. https://doi.org/10.1007/s10661-021-09518-9

Fetter, C. W. (1994). *Applied hydrogeology* (3rd ed., p. 600). Upper Saddle River: Prentice Hall Inc.

Freeze, R. A., Cherry, J. A., 1979. '*Groundwater*', prentice hall Inc. Englewood Cliffs, New Jersey.p.7

George, N. J., Obinawu, V. I., Udofia, K. M., 2011. Estimation of Aquifer Hydraulic Parameters via Complementing Surficial Geophysical Measurement by Laboratory Measurements on the Core Samples in Southern part of Akwa Ibom State, Nigeria. *Int Rev Phys*, Praise Worthy Prize, Italy 5(2):88–97

George, N. J., Ekanem, A. M., Ibanga, J. I. & Udosen, N.1., 2017. Hydrodynamic Implications of Aquifer Quality Index (AQI) and Flow Zone Indicator (FZI) in groundwater abstraction: a case study of coastal hydro-lithofacies in South-eastern Nigeria. *J Coast Conserv*., 21, 759 - 776, https://doi.org/10.1007/s11852-017-0535-3

George, N. J., Emah, J. B., & Ekong, U. N. 2015. Geohydrodynamic properties of hydrogeological units in parts of Niger Delta, Southern Nigeria. Journal of African Earth Sciences, 105, 55–63

Ibanga, J. I., George, N. J., 2016. Estimating geohydraulic parameters, protective strength, and corrosivity of hydrogeological units: a case study of ALSCON, Ikot Abasi, southern Nigeria. Arabian Journal of Geoscience, 9, Pp. 363. https://doi.org/10.1007/s12517-016-2390-1.

Ibuot, J. C. and Obiora, D. N., 2020. Estimating geohydrodynamic parameters and their implications on aquifer repositories: a case study of university of Nigeria, Nsukka, Enugu State. *Water Practice & Technology*, 16(1), 162 – 182. https://doi: 10.2166/wpt.2020.105.

Kouassi, F. W., Kouassi, K. A., Coulibaly, A., Kamagaté, B., & Savané, I. 2017. Efficiency of Inverse Slope Method in the Interpretation of Electrical Resistivity Soundings Data of Schlumberger Type. International Journal of Engineering & Science Research, 7, 121-130

Kruseman , G. P., de Ridder, N. A., 1990. Analysis and Evaluation of Pumping Test Data. Bulletin 11, Institute for Land Reclamation and Improvement, Wageningen, 41 – 46.

Lobo Ferreira, J.P., Chachadi, A.G., Diamantino, C., Henriques, M. J., 2005. Assessing Aquifer vulnerability to sea-water intrusion using GALDIT method: part I application to the Portuguese Aquifer of Monte Gordo. The Fourth Inter Celtic Colloquium on Hydrology and Management of Water Resources, Guimaraes, Portugal, July 11–14, 2005, pp. 1–12.

Mbipom, E. W., Okwueze, E. E. & Onwuegbeche, A. A. A., 1996. Estimation of transmissivity using VES data from Mbaise area of Nigeria. *Nigerian Journal of Physics*, 85, 28-32.

Niwas, S., Tezkan, B., & Israil, M., 2011. Aquifer hydraulic conductivity estimation from surface geoelectrical measurements for Krauthausen test site, Germany. *Hydrogeology Journal*, 19, 307–315

Okereke, C. S., Esu, E. O. & Edet, A. E., 1998. Determination of groundwater sites using geological and geophysical techniques in the Cross River State, southeastern Nigeria. *Journal of African Earth Sciences*. 27(1), 149-163.

Reijers, T. J. A. & Petters, S. W. 1987. Depositional environments and diagenesis of Albian Carbonates on the Calabar Flank, SE Nigeria. *Journal of Petroleum Geology*, 10(3), 283-294.

Bouadou, R. A. M., Kouassi, K. A., Kouassi, F. W., Coulibaly, A. and Gnagne, T., 2019. Use of the Inverse Slope Method for the Characterization of Geometry of Basement Aquifers: Case of the Department of Bouna (Ivory Coast). Journal of Geoscience and Environment Protection, **7**, 166-183

Sankarnaryan, P. V., Ramanujachary, K. R., 1967. An Inverse Slope Method for determining absolute Resistivities. Geophysics; **32**(6): 1036-1040

Sattar, G. S., Keramat, M. and Shahid, S., 2016. Deciphering transmissivity and hydraulic conductivity of the aquifer by vertical electrical sounding (VES) experiments in Northwest Bangladesh. *Appl Water Sci* **6,** 35–45 https://doi.org/10.1007/s13201-014-0203-9

Short, K. C. and Stauble, A. J. (1967). Outline Geology of the Niger Delta. *AAPG Bull.*, 51; 761-779.

Soupios P.M., Kouli M., Valliantos F., Vafidis A., Stavroulakis G., 2005. Estimation of aquifer hydraulic parameters from surficial geophysical methods: a case study of Keritis Basin in Chania (Crete-Greece). *J. Hydrol*., 338, 122–13

Uwa, U. E., Akpabio, G. T. and George, N. J. 2018. Geohydrodynamic Parameters and Their Implications on the Coastal Conservation: A Case Study of Abak Local Government Area (LGA), Akwa Ibom State, Southern Nigeria. *Natural Resources Research*, https://doi.org/10.1007/s11053-018-9391-6